

## Analysis and Comparison of Closed System Based Thermal Cycles Undergoing Different Polytropic Transformations

Ramon Ferreiro. Garcia<sup>1</sup>, Jose Carbia Carril<sup>2</sup>

<sup>1</sup>Ind. Eng. Dept., <sup>2</sup> Energy & Propulsion Dept

<sup>2</sup>University of A Coruna, ETSNM, Paseo de Ronda 51, 15011, A Coruna, Spain.

**\*Corresponding Author:** Ramon Ferreiro. Garcia, Ind. Eng. Dept University of a Coruna, ETSNM, Paseo de Ronda 51, 15011, a Coruna, Spain

### ABSTRACT

This research work deals with a feasible thermal energy convertor consisting of a non-regenerative thermal cycle, composed by two closed polytropic transformations and two closed isochoric transformations which are implemented by means of a double effect reciprocating cylinder which differs basically from the Carnot based conventional thermal cycles in that:

- All cycle processes undergoes closed transformations, instead of the conventional open processes of the Carnot based thermal cycles,
- In the active processes of this cycle (polytropic path functions), as heat is being absorbed or rejected under load-dependent path functions, mechanical work is simultaneously performed, avoiding the conventional quasi-adiabatic expansion or compression processes inherent to the Carnot based engines and,
- During the load-dependent path functions of the closed polytropic processes of this cycle, mechanical work is also performed by means of the working fluid contraction due to heat rejection.

An analysis of the proposed cycle is carried out for helium working fluids and results are compared with those of a Carnot engine operating under the same ratio of temperatures. Because of the cycle analysis, it follows that the ratio of top to the bottom cycle temperatures has very low dependence on the ideal thermal efficiency, but the specific work. Furthermore, within the range of relative low operating temperatures, high thermal efficiency is achieved, even exceeds the Carnot factor when it operates with a thermal working fluid such as helium.

**Keywords:** Carnot factor, Closed transformations, Load-dependent path functions, Polytropic processes, Thermal efficiency.

Nomenclature		Acronyms	
$\gamma$	adiabatic expansion coefficient	C	constant value parameter
$n$	polytropic expansion coefficient	CF	Carnot factor = Carnot efficiency
$\eta$	thermal efficiency	CR	heat conversion ratio
$\eta_{23}$	thermal efficiency of process (2)-(3)	EES	Engineering Equation Solver
$C_p$	specific heat at constant pressure (kJ/kg-K)	GWP	global warming potential
$C_v$	specific heat at constant volume(kJ/kg-K)	NCTC	non-Carnot thermal cycle
$v$	specific volume ( $m^3/kg$ )	NORC	non-Organic Rankine cycle
$W$	specific work (kJ/kg)	ORC	organic Rankine cycle
$h$	specific enthalpy (kJ/kg)	PI	polytropic index
$u$	specific internal energy (kJ/kg)		
$p$	pressure (bar)		
$s$	specific entropy (kJ/kg-K)		
$T$	temperature (K)		
$q_o$	heat rejected by the cycle (kJ/kg)		
$q_i$	heat supplied to the cycle (kJ/kg)		
$R$	universal constant of ideal gases (kJ/kg-K)		

INTRODUCTION

Almost all known thermal cycles so far rely on the Carnot cycle, meaning quadrilateral cycles in which ideally, heat is absorbed at constant temperature (top temperature) and work is delivered when temperature decreases from the top temperature to approach the bottom temperature under a quasi entropic transformation. The power cycles that obey this model are classified in two main groups based on the nature of the working fluid: gas power cycles and vapour power cycle. The difference between the two groups is that, in the first case, the working fluid is gaseous and does not experiment any phase change, while for the second group, there is a liquid-vapour phase change process of the working fluid within the cycle. In Fig.1 a simple classification of heat engine based cycles is depicted.

Some studies regarding trilateral thermal cycles have recently appeared in scientific literature. Thus, for instance, a comparison of trilateral NCTCs and organic Rankine cycles has been

carried out by [1] in which a clear contribution to the thermal efficiency enhancement has been reported. Nevertheless, in the work presented in this paper, a different perspective regarding the conventional trilateral and quadrilateral thermal cycles is considered. Such characteristic differences are depicted in Fig.1, which exhibit some properties inherent to the NCTC, summarised as:

- Load reaction driven path functions along the active stroke of the double effect cylinder,
- Operates under closed non-regenerative thermal processes,
- Performs mechanical work by expansion-contraction polytropic path functions, and
- Thermal efficiency quasi-independent of the cycle temperatures

Since the thermal efficiency of the Carnot based engine at very low top temperature tends to zero, it follows that under such conditions, the proposed cycle could surpass the limits stated by the Carnot statement.

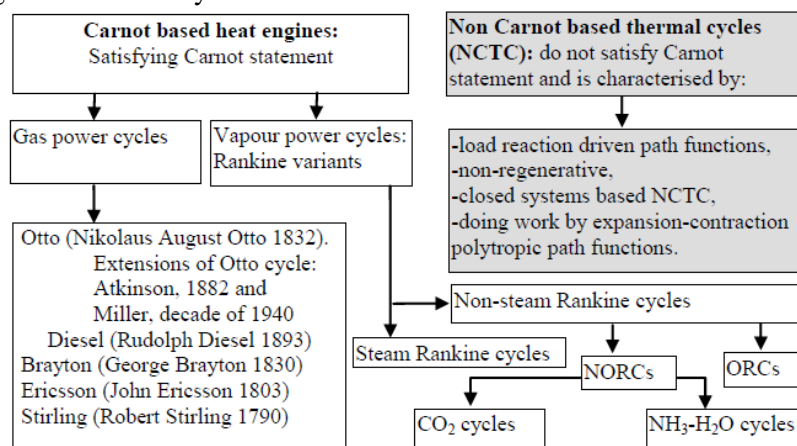


Fig1. Classification of commonly thermal cycles (Carnot and non-Carnot based thermal engines)

The objective of the study is to efficiently convert low temperature heat from renewable thermal sources and heat rejected from various industrial sources and cooling systems, which may include but is not limited to geothermal, ocean thermal and direct solar thermal sources, heat rejected from Diesel cooling systems (air, lube oil and jacket water coolers), and residual flue gases, as well bottoming steam Rankine condensers, to be converted by means of the proposed thermal cycle and plant structure into electric energy. The proposed conversion method is based on a different thermodynamic cycle: the non condensing mode trilateral thermal cycle with or without regeneration. The proposed cycle is not based on the quadrilateral

Carnot cycle but on the trilateral cycle which absorbs heat and performs mechanical work simultaneously between states (2) and (3) of Fig. 3. As a consequence of this contribution, this cycle is not restricted by the CF constraints. Its maximum thermal efficiency is influenced not only by the ratio of the top to bottom temperatures like, for instance, in the cycles' analysis described in [2], [3], but also by some factors such as the characteristics of the working fluids and regeneration capabilities when regeneration is considered. In the low temperature range, bottoming ORCs constitute another viable option, having shown good thermodynamic performance for low top temperature of the bottoming cycles [4], [5] and [6].

## Analysis and Comparison of Closed System Based Thermal Cycles Undergoing Different Polytropic Transformations

The organic working fluids for residual heat applications with low temperature ORCs due to their thermal efficiency have gained importance for several different applications such as: renewable energy and low temperature heat recovery [7], and [8] as the most relevant. The proposed heat conversion procedure is based on a non-conventional thermodynamic cycle which differs from the Carnot based cycles in that:

- All cycle transformations are performed undergoing closed system transformations, instead of the conventional open transformations inherent to the Carnot based thermal cycles and
- In all active processes of this cycle, as heat energy is being absorbed, undergoing a polytropic load-dependent path function, mechanical work is simultaneously performed, avoiding the conventional quasi-adiabatic expansion processes of the Carnot based engines. Because of this contribution, this cycle is not restricted by the CF constraints. Its maximum thermal efficiency is not influenced by the ratio of the top to bottom temperatures. As consequence, this cycle is not efficient at medium and high temperatures. However, at low temperatures it can surpass the Carnot factor according to a recently published work consisting of an inverse Rankine cycle proposed by [9], in which the Carnot Factor has been surpassed. The authors showed that the proposed hybrid vapor compression refrigeration system achieves significantly higher COP than a conventional vapor compression refrigeration system, and even higher than the *reverse*

*Carnot cycle* at the same operation conditions.

### Analysis of the Some Ideal Thermodynamic Transformations

In order to focus attention on the closed thermal processes that could take place in such thermal cycles, this section deals with the ideal transformations in terms of mechanical work that could be carried out in closed process based NCTCs. In this way, the fact of introducing the concept of displacement work undergoes the movement of the piston in a cylinder from position  $i$  to position  $i+1$ , while volume changes from  $V_i$  to  $V_{i+1}$ , causing an amount of  $W$  (mechanical work) done by the system which is given as

$$W_{i \rightarrow i+1} = \int_{V_i}^{V_{i+1}} p \cdot dV$$

The amount of work done is given by the area under the process (i) – (i+1) shown in the diagram of Fig. 2. In order to analyse the ideal closed thermodynamic cases aimed at the mechanical work done, let's consider the displacement of a piston into its cylinder under different path functions as shown in Fig. 2, which undergoes different realisable path functions designed as

- Isobaric process (pressure ,constant at constant load), Fig 2(a)
- Polytropic process (  $pV^n = C$ , with  $C$ , constant), Fig 2(b)
- Adiabatic process (  $pV^\gamma = C$ , with  $C$ , constant), Fig 2(c)

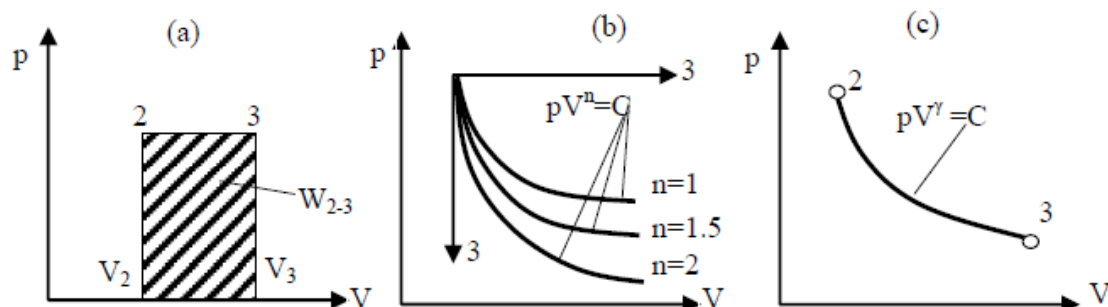


**Fig2.** Mechanical work performed under different thermodynamic processes when evolving from state point (i) to state point (i+1), denoted as state point (2) and state point (3) respectively. (a), isobaric path-function. (b), polytropic path function, and (c), adiabatic path function.

The work done under isobaric transformations  $PI=0$ , Fig. 2(a)

$$W_{1-2} = \int_{V_1}^{V_2} p \cdot dV = p \cdot (V_2 - V_1) \quad (1)$$

The mechanical work delivered under an isobaric process where  $n=0$  is

The work done under polytropic transformations,  $PI = n$ , Fig. 2(b)

## Analysis and Comparison of Closed System Based Thermal Cycles Undergoing Different Polytropic Transformations

The polytropic transformation obey  $p \cdot V^n = p_1 \cdot V_1^n = p_2 \cdot V_2^n = p_3 \cdot V_3^n = C$ .

Consequently, the pressure at any intermediate point of the polytropic transformation is

$$p_i = \frac{p_2 \cdot V_2^n}{V_i^n} = \frac{p_1 \cdot V_1^n}{V_i^n} = \frac{p_3 \cdot V_3^n}{V_i^n} = \frac{p_x \cdot V_x^n}{V_i^n} \quad (2)$$

The mechanical work delivered under a polytropic process when evolving from a point (2) to point (3) is determined as follows

$$W_{2-3} = \int_{V_2}^{V_3} p \cdot dV = \int_{V_2}^{V_3} \frac{p_2 \cdot V_2^n}{V^n} dV = \frac{p_3 \cdot V_3 - p_2 \cdot V_2}{1-n} = \frac{R \cdot (T_3 - T_2)}{1-n} \quad (3)$$

The mechanical work done under adiabatic transformations,  $PI = \gamma$ , Fig. 2(c)

The mechanical work delivered undergoing adiabatic path function, where  $n = \gamma$ , is determined as follows:

The adiabatic transformation obey  $p \cdot V^\gamma = p_1 \cdot V_1^\gamma = p_2 \cdot V_2^\gamma = p_3 \cdot V_3^\gamma = C$

Consequently, the pressure at any point of the adiabatic transformation is

$$p_i = \frac{p_2 \cdot V_2^\gamma}{V_i^\gamma} = \frac{p_1 \cdot V_1^\gamma}{V_i^\gamma} = \frac{p_3 \cdot V_3^\gamma}{V_i^\gamma} = \frac{p_x \cdot V_x^\gamma}{V_i^\gamma} \quad (4)$$

Where,  $\delta Q$  or  $dQ = 0$  and the adiabatic exponent  $\gamma = \frac{C_p}{C_v}$

Since  $\delta Q = dU + dW = 0$ , then

$$dW = dU = -C_v \cdot dT$$

$$dW = p \cdot dV$$

with

$$p_2 \cdot V_2^\gamma = p_3 \cdot V_3^\gamma = C$$

The mechanical work delivered under an adiabatic process when evolving from a point (2) to point (3) is determined as follows

$$W_{2-3} = \int_{V_2}^{V_3} \frac{C}{V^\gamma} dV = C \int_{V_2}^{V_3} V^{-\gamma} dV = \frac{p_3 V_3 - p_2 V_2}{1-\gamma} = \frac{R \cdot (T_3 - T_2)}{1-\gamma} \quad (5)$$

Obviously, the single ideal closed process based transformations above described above may be only useful if they can be implemented into a thermal cycle. In this purpose, the following sub-section deals with such topic.

### The Energy Conversion Ratio for Closed Processes

The thermal efficiency of a single closed thermodynamic transformation, also called the

energy (conversion ratio)  $C_R$  which is the inverse of the heat transfer ratio, is defined as the ratio of the work done to the heat absorbed during a thermodynamic transformation. Thus, considering transformation (2)-(3) of Fig. 2(a) undergoing an *isobaric* path function, for which  $PI = 0$ , according to the first principle applied to closed processes, it follows that the mechanical work is

$$W_{23} = q_{23} - \Delta u_{23} \quad (6)$$

Then the  $C_R$  or process efficiency of this closed reversible transformation (2)-(3) for an isobaric path function yields

$$C_R = \eta_{23} = \frac{W_{23}}{q_{23}} = \frac{q_{23} - \Delta u_{23}}{q_{23}} = 1 - \frac{\Delta u_{23}}{q_{23}} = 1 - \frac{C_v \cdot (T_3 - T_2)}{C_p \cdot (T_3 - T_2)} = 1 - \frac{1}{\gamma} \quad (7)$$

Considering a *polytropic* path function, so that  $PI = n$ , then, the conversion ratio of this closed reversible transformation (2)-(3) shown in Fig. 2 (b) yields

$$C_R = \eta_{23} = \frac{W_{23}}{q_{23}} = \frac{q_{23} - \Delta u_{23}}{q_{23}} = 1 - \frac{\Delta u_{23}}{q_{23}} = 1 - \frac{\Delta u_{23}}{W_{23} + \Delta u_{23}} = 1 - \frac{C_v \cdot (T_3 - T_2)}{C_v \cdot (T_3 - T_2) + \frac{R \cdot (T_3 - T_2)}{1-n}} = 1 - \frac{(1-n) \cdot C_v}{C_p - n \cdot C_v} = \frac{C_p - C_v}{C_p - n C_v} = \frac{\gamma - 1}{\gamma - n} \quad (8)$$

Since the mechanical work is

$$W_{2-3} = \int_{V_2}^{V_3} \frac{C}{V^\gamma} dV = \frac{p_3 V_3 - p_2 V_2}{1-\gamma} = \frac{R \cdot (T_3 - T_2)}{1-\gamma}$$

Considering an *adiabatic* path function, so that  $PI = \gamma$ , then, the conversion ratio of this closed reversible transformation (2)-(3) shown in Fig. 2 (c) yields

$$C_R = \eta_{23} = \frac{W_{23}}{q_{23}} = \frac{q_{23} - \Delta u_{23}}{q_{23}} = 1 - \frac{\Delta u_{23}}{q_{23}} = 1 - \frac{\Delta u_{23}}{W_{23} + \Delta u_{23}} = 1 - \frac{C_v \cdot (T_3 - T_2)}{C_v \cdot (T_3 - T_2) + \frac{R \cdot (T_3 - T_2)}{1-\gamma}} = 1 - \frac{(1-\gamma) \cdot C_v}{C_p - \gamma \cdot C_v} = \frac{C_p - C_v}{C_p - \lambda C_v} = \frac{\gamma - 1}{\gamma - \gamma} = \infty \quad (9)$$

Since the mechanical work done is

$$W_{2-3} = \int_{V_2}^{V_3} \frac{C}{V^\gamma} dV = \frac{p_3 V_3 - p_2 V_2}{1-\gamma} = \frac{R \cdot (T_3 - T_2)}{1-\gamma}$$

Where, the amount of heat interchanged with the closed adiabatic process (adiabatic expansion or contraction processes) during the transformation is zero, so that the result achieved by (9) is coherent with the adiabatic transformation. The required heat absorbed by the gas to perform an adiabatic transformation must be accounted to the previous process consisting of a heating process without performing work.

Surprisingly, expressions (7), (8) and (9) defining the  $C_R$ , ideally exhibit total

## Analysis and Comparison of Closed System Based Thermal Cycles Undergoing Different Polytropic Transformations

independence of the temperature. This suggests to us that since the Carnot factor tends to zero as the ratio of top to bottom temperatures approaches unity, for low top temperatures, Carnot efficiency is lower than the value of this  $C_R$ , since, as stated before, when the top

temperature approaches the bottom temperature,  $CF$  tends towards zero. Thus, thermal cycles that involve transformations in which heat is absorbed and work is developed simultaneously do not obey the Carnot statement.

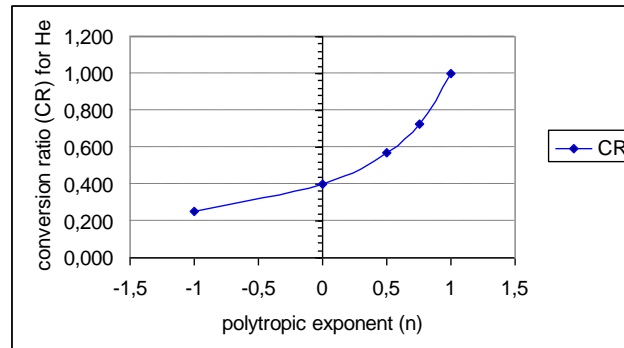


**Fig3.** The conversion ratio for different PI values

Considering an approach to ideal gases such as helium, the corresponding conversion ratio definition undergoing an isobaric transformation, for which  $PI = 0$  yields  $C_R = 0.4$  as shown in (10), matches the conversion ratio represented in Fig. 3 for a  $PI = 0$

$$C_R = \eta_{23} = \frac{W_{23}}{q_{23}} = 1 - \frac{1}{\gamma_{He}} = 1 - \frac{1}{1.665} = 0.4 \quad (10)$$

The conversion ratio as function of the  $PI$  values ranging from -1.5 to 1.5 is depicted in Fig. 3. It is observed that for a  $PI$  value of zero, the  $C_R$  is 0.4, which matches the value yielded by (10). In the same way, for a  $PI$  value of zero which is the case of an isothermal transformation, the  $C_R$  is one, since all transferred heat is converted into work and vice-versa, undergoing constant internal energy.

### The Analysis of Heating and Cooling Processes Undergoing Closed System Transformations Following Isobaric Quasi-Reversible Path Functions

A quasi-reversible process is depicted in the Fig. 4, although all actual processes are irreversible

because in nature, such spontaneous transformations do not occur. In Fig. 4, it is considered a specific amount of gaseous working fluid enclosed in a piston-cylinder arrangement is considered. The weight on the piston fixes the pressure in the cylinder as heat is added to or extracted from the system. At the initial state (2), the working fluid is compressed at supercritical pressure  $p_2$  and temperature  $T_2$ . The reader might envision that a heat source and heat sink devices could be used as a heater and cooler respectively.

The added heat energy results in an increase in the temperature of the fluid, while the fluid expands at constant pressure, causing the changing of state from point (2) to an intermediate point lower than point (3). Continuing with further addition of heat, the working fluid is converted from supercritical cold fluid into supercritical and superheated hot gas. At state (3), the transformation is complete, and all the cold supercritical fluid has turned to hot supercritical superheated gas at temperature  $T_3$ .

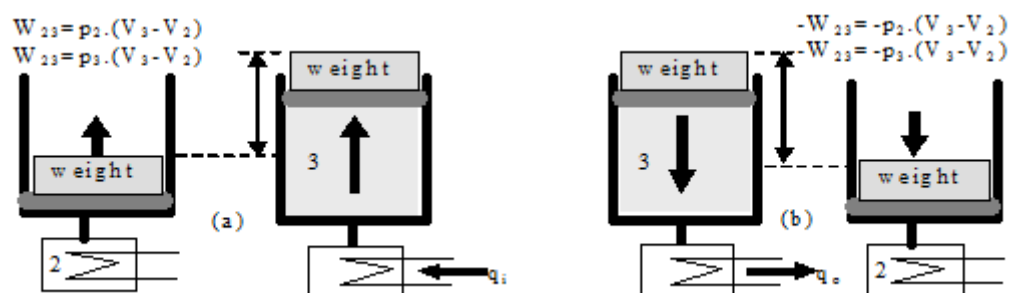


**Fig4.** The process of heating and cooling a fluid at constant pressure (closed process) as an approach to a reversible process, where fluid is confined into a heater and a cylinder, as heat is being added.

## Analysis and Comparison of Closed System Based Thermal Cycles Undergoing Different Polytropic Transformations

Assuming that the heating process was conducted quasi-statically, path (2)-(3) is a collection of equilibrium states following an isobar (a line of constant pressure). The experiment could be repeated with lesser or greater weight on the piston (i.e., at lower or higher pressures).

When considering an approach to a reversible process, the reversible closed system energy balance applied on the closed system shown in Fig. 4, when changing from point (2) to point (3), undergoing isobaric path functions it states that

$$q_{23} - W_{23} = \Delta u_{23} + mg\Delta z_{23} + K\Delta E_{23} \quad (11)$$

Assuming that potential and kinetic energies can be neglected, then (1) can be stated as

$$q_{23} - W_{23} = \Delta u_{23} \quad (12)$$

Consequently, the supplied heat at constant pressure along transformation (2)-(3) is also defined as

$$q_{23} = (u_3 - u_2) + p_2 \cdot (V_3 - V_2)$$

Where, two simultaneous modes of energy absorption take place along process (2)-(3):

- increasing internal energy in  $u_3 - u_2$
- performing mechanical work in  $p_2 \cdot (V_3 - V_2) = p_3 \cdot (V_3 - V_2)$

$$(13)$$

When dealing with isobaric closed process analysis, thermodynamic equilibrium of a

The amount of heat transferred to the system at constant pressure to evolve from state (2) to state (3) (isobaric expansion) is defined as

$$q_{23} = \Delta h_{23} = C_p \Delta T_{23} = \Delta u_{23} + W_{23} = u_3 - u_2 + p_2 \cdot (V_3 - V_2) \quad (14)$$

The change in state from (2) to (3) is significant. Along this process an amount of mechanical work  $W_{23}$  is performed, which is quantified as

$$W_{23} = \int_{V_2}^{V_3} p_2 \cdot dv = p_2 \cdot (V_3 - V_2) \quad (15)$$

Continuing with the cycle evolutions, the amount of heat transferred from the system to the heat sink at constant pressure (isobaric compression) to evolve from state (3) to state (2) is defined as

$$-q_{23} = -\Delta h_{23} = -C_p \Delta T_{23} = -\Delta u_{23} - W_{23} = -(u_3 - u_2) - p_2 \cdot (V_3 - V_2) \quad (16)$$

The change in state from (3) to (2) is similar to the previous. Along this process, mechanical work  $W_{23}$  was performed on the isobaric compression process, which is quantified as

$$-W_{23} = -\int_{V_2}^{V_3} p_2 \cdot dv = -p_2 \cdot (V_3 - V_2) \quad (17)$$

Fig. 4(c) and Fig. 4(g) depict the p-V and T-s diagrams showing the series of infinitesimal state changes along the isobaric expansion occurring between states (2)-(3), and isobaric compression (3)-

system is very difficult to be realised during the occurrence of a thermodynamic process. Thermal systems of the industrial processes do not attain thermodynamic equilibrium, therefore only certain assumptions make it akin to a system in equilibrium for the sake of analysis.

Quasi-static refers to “almost static”, associated to the slowness of the occurrence of a process. This is the basic assumption for attaining near equilibrium of a system. It is considered that the change in state occurs at an infinitely slow pace, thus consuming very long time for completion of the process. Thus, quasi-static processes are considered to remain in thermodynamic equilibrium. A paradigmatic example of a quasi-static process is depicted in Fig. 4, consisting of a confined fluid which is heated and cooled at constant pressure into a cylinder.

To explain the behaviour of the processes carried out during a cycle in which heat is absorbed, a fraction of the absorbed heat is converted to mechanical work and the rest is rejected, let us consider the locating of a working fluid (gas) in a single effect cylinder with a certain load kept on the piston, as shown in Fig. 5(a). The gas at state point (2) attains the equilibrium conditions defined by  $p_2$ ,  $V_2$ ,  $T_2$ ,  $s_2$  and  $u_2$ . After a certain amount of heat is added to the gas, it is found that the piston becomes displaced, reaching state point (3) shown in Fig. 4(b), so that the state point conditions are  $p_3$ ,  $V_3$ ,  $T_3$ ,  $s_3$  and  $u_3$ .

## Analysis and Comparison of Closed System Based Thermal Cycles Undergoing Different Polytropic Transformations

(2) completing a cycle. The net work performed during the cycle according to the first principle must satisfy  $W_{23} - W_{23} = 0$ .

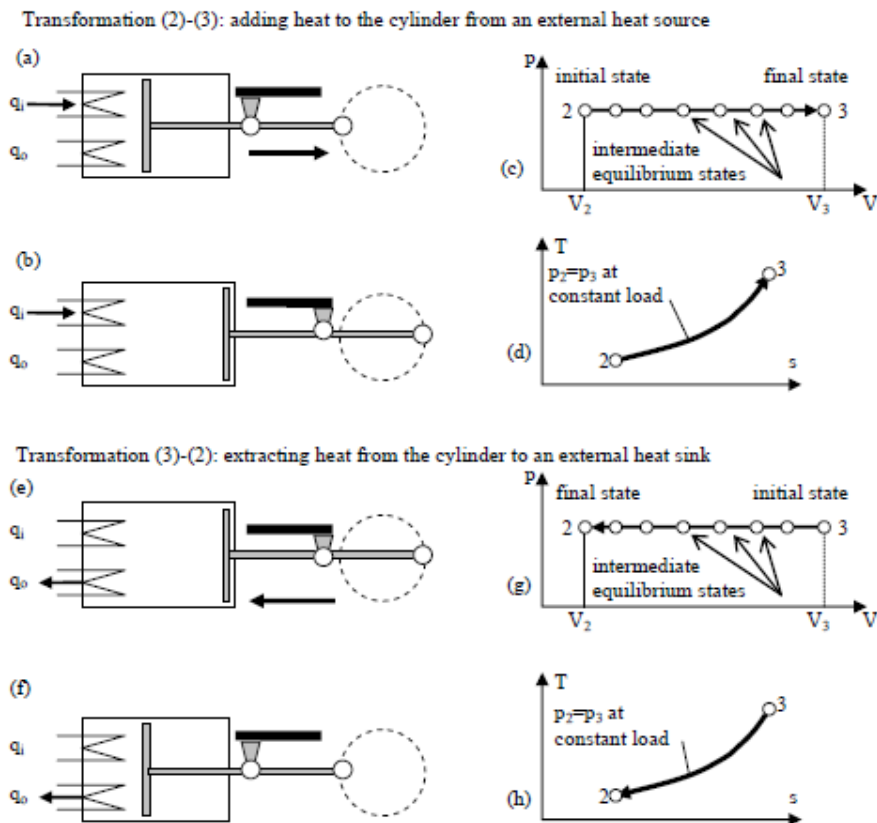


**Fig5.** Quasi-static process: A succession of intermediate equilibrium states at constant pressure when adding or extracting heat to and from a cylinder.

### THE ANALYSIS OF CLOSED SYSTEM BASED SINGLE EFFECT THERMAL CYCLES UNDERGOING ISOBARIC PATH FUNCTIONS

The analysis of a cycle undergoing net mechanical work is under analysis. Thus, with regard to the thermal efficiency of the closed

transformation based cycle, it will be demonstrated that the thermal efficiency depends largely on the adiabatic expansion coefficient, while the specific work depends on the cycle temperatures. The analyses of the closed system based cycle are depicted in Fig. 6.

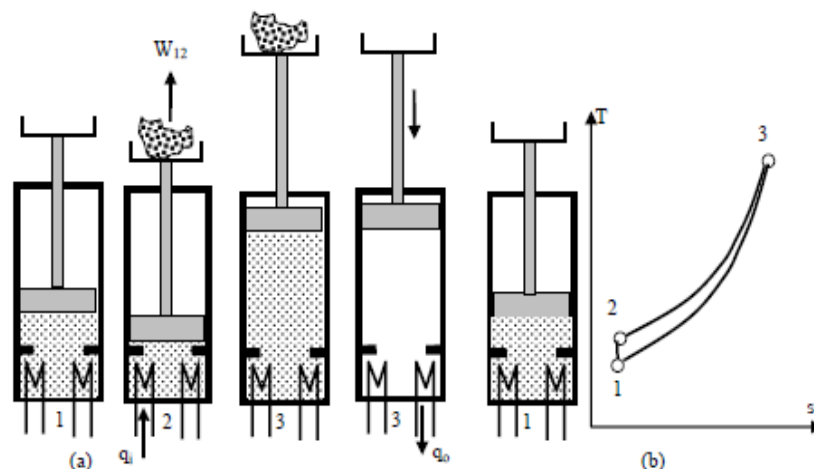


**Fig6.** A thermal cycle composed of closed system transformations. (a), a trilateral NCTC consisting of a cylinder that absorbs heat  $q_1$ , delivering work simultaneously along transformation (2)-(3) and rejecting heat during transformation (3)-(1). (b), the T-s diagram of the trilateral NCTC. At constant load, the pressure is constant which results in the heating process undergoing an isobaric path function.

## Analysis and Comparison of Closed System Based Thermal Cycles Undergoing Different Polytropic Transformations

Considering a cycle composed of closed system based transformations of single effect (that is, loaded only along transformation (2)-(3) and unloaded along transformation (3)-(1). This cycle is characterised by its ability to perform useful mechanical work while simultaneously absorbing heat. Therefore, assuming the trilateral NCTC composed of closed system transformations as shown in Fig. 4 (a) and Fig. 5 (b) it follows that the supplied heat from an external power source is

$$q_i = \Delta u_{32} + W_{23} = u_3 - u_2 + p_2 \cdot (v_3 - v_2) = C_v(T_3 - T_2) + R \cdot (T_3 - T_2) = C_p \cdot (T_3 - T_2) \quad (18)$$

The rejected heat to the heat sink is

$$q_o = \Delta u_{31} + W_{31} = u_3 - u_1 + p_1 \cdot (v_3 - v_1) = C_v \cdot (T_3 - T_1) \quad (19)$$

since  $W_{31} = p_1 \cdot (v_3 - v_1) = 0$

Thus the thermal efficiency is

$$\eta = \frac{q_i - q_o}{q_i} = 1 - \frac{q_o}{q_i} = 1 - \frac{u_3 - u_1}{u_3 - u_2 + p_2 \cdot (v_3 - v_2)} = 1 - \frac{C_v \cdot (T_3 - T_1)}{C_p \cdot (T_3 - T_2)} = 1 - \frac{1}{\gamma} \cdot \frac{(T_3 - T_1)}{(T_3 - T_2)} \quad (20)$$

From (10) it follows that as  $T_2$  increases, due to the increasing of pressure ratio, the thermal efficiency decreases accordingly. From (7) it follows also that the maximum theoretical thermal efficiency is achieved when  $T_2$  approaches  $T_1$  since

$$\lim_{T_2 \rightarrow T_1} (\eta) = \lim_{T_2 \rightarrow T_1} \left[ 1 - \frac{1}{\gamma} \cdot \frac{(T_3 - T_1)}{(T_3 - T_2)} \right] = 1 - \frac{1}{\gamma} \quad (21)$$

Assuming an approach to ideal gasses such as helium, the maximum achievable efficiency is approached as  $\eta_{he} = 1 - \frac{1}{\gamma} = 1 - \frac{1}{1.665} = 0.4$  for helium

as working fluid, and for any temperature  $T_3 > T_2 > T_1$

Considering now the same cycle composed of closed system transformations, as shown in Fig. 7 (a) and Fig. 7 (b), where transformation (3)-(4) corresponds to the process of system unloading (which is an isentropic expansion or contraction), it follows that the supplied heat from an external power source is

$$q_i = \Delta u_{32} + W_{23} = u_3 - u_2 + p_2 \cdot (v_3 - v_2) = C_v(T_3 - T_2) + R \cdot (T_3 - T_2) = C_p \cdot (T_3 - T_2) \quad (22)$$

The rejected heat to the heat sink is

$$q_o = \Delta u_{41} - W_{41} = u_4 - u_1 - p_1 \cdot (v_4 - v_1) \quad (23)$$

where

$$W_{23} = p_2 \cdot (v_3 - v_2) = R \cdot (T_3 - T_2) \quad \text{and}$$

$W_{41} = 0$ , since along this transformation, the cylinder is unloaded.

Thus, the thermal efficiency is

$$\eta = \frac{q_i - q_o}{q_i} = 1 - \frac{q_o}{q_i} = 1 - \frac{C_v \cdot (T_4 - T_1)}{C_p \cdot (T_3 - T_2)} = 1 - \frac{1}{\gamma} \cdot \frac{(T_4 - T_1)}{(T_3 - T_2)} \quad (24)$$

consisting of a cylinder that absorbs heat  $q_i$  along states (2)-(3), simultaneously delivering mechanical work, and rejecting heat along the transformation (4)-(1). (b), the T-s diagram of the quadrilateral cycle. At constant load, the pressure is constant so that the heating process undergoes an isobaric path function.

According to the results of both analysed cycles, an important amount of heat supplied to cycle  $q_i$  is rejected as  $q_o$ . Another thermal engine structure, composed of closed system based transformations for which the cooling phase is carried out by simultaneously performing useful mechanical work is possible. The topic analysed in the next section deals with such concept.

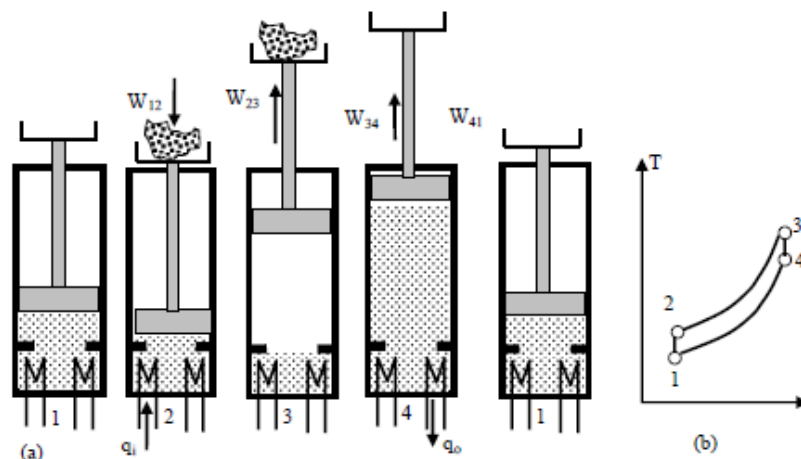


Fig7. A thermal cycle composed of closed systems transformations. (a), the quadrilateral cycle

**Closed System Based Double Effect Thermal Cycle Analysis under Isobaric Path Functions**

In order to apply a technique on closed system based transformations in which the cooling phase the heat rejection phase is carried out by simultaneous performing useful mechanical work, the thermal cycle depicted in Fig. 8 is analysed.

The quadrilateral cycle depicted with Fig. 8 consists of a cylinder that absorbs heat  $q_i$

The supplied heat from an external power source is

$$q_i = \Delta u_{32} + W_{23} = u_3 - u_2 + p_2 \cdot (v_3 - v_2) \tag{25}$$

The rejected heat to the heat sink is

$$q_o = \Delta u_{56} - W_{56} = u_5 - u_6 - p_5 \cdot (v_5 - v_6) \tag{26}$$

Thus the thermal efficiency is

$$\eta = \frac{q_i - q_o}{q_i} = 1 - \frac{q_o}{q_i} = 1 - \frac{u_5 - u_6 - p_5 \cdot (v_5 - v_6)}{u_3 - u_2 + p_2 \cdot (v_3 - v_2)} = 1 - \frac{2 - \gamma}{\gamma} \cdot \frac{T_5 - T_6}{T_3 - T_2} \tag{27}$$

between state points (2) and (3), performing mechanical work. Also, it rejects heat along transformation (5)-(6) while delivering simultaneously mechanical work. The transformations carried out are shown in T-s and v-V diagrams 8(b) and 8(c). At constant load, the pressure is constant so that the heating and cooling processes undergo isobaric path functions while transformations (3)-(4) and (6)-(2) are isentropic path functions.

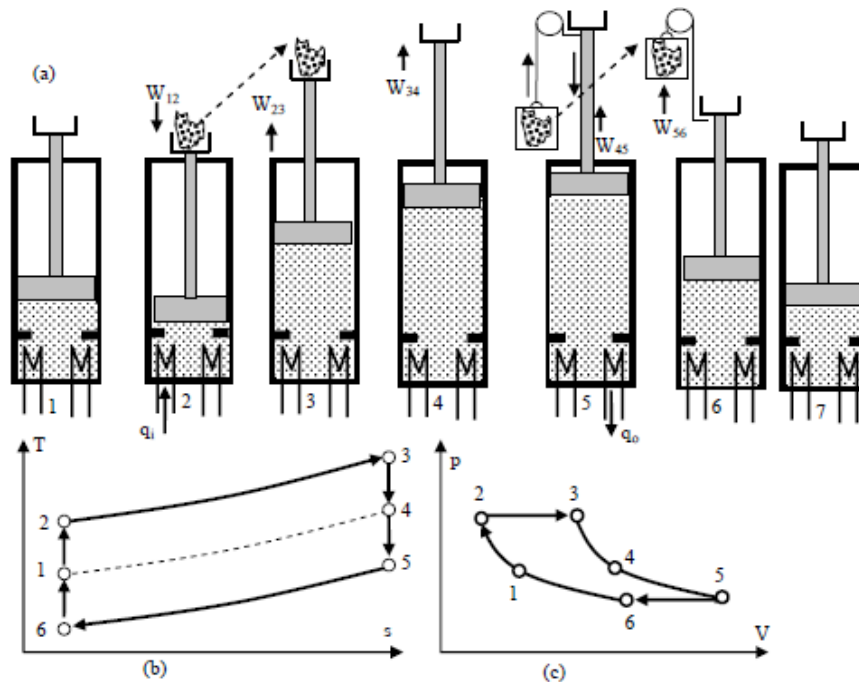


**Fig8.** Closed system based double effect thermal cycle. (a), the structure of a single effect piston- cylinder engine. (b), the T-s diagram of the quadrilateral cycle. (c), p-v diagram of the quadrilateral cycle.

Once a thermal cycle undergoing isobaric active processes has been described, the next section deals with a case study applied to a thermal cycle undergoing active closed polytropic path functions.

**A CASE STUDY**

In this section a case study dealing with a NCTC consisting of a closed systems based thermal

cycle is described and analysed with the help of Fig 9. It is based on a double effect cylinder which drives a crankshaft as the mechanical power converter. The double effect cylinder operates with the selected working fluid which is heated and cooled by means of an external heat source and heat sink. Cycle modelling is carried out with data extracted from [7], according to the selected working fluids, using the computational tool EES, (Engineering

Equation Solver), where the used data belongs to REFPROP, referenced as [10].

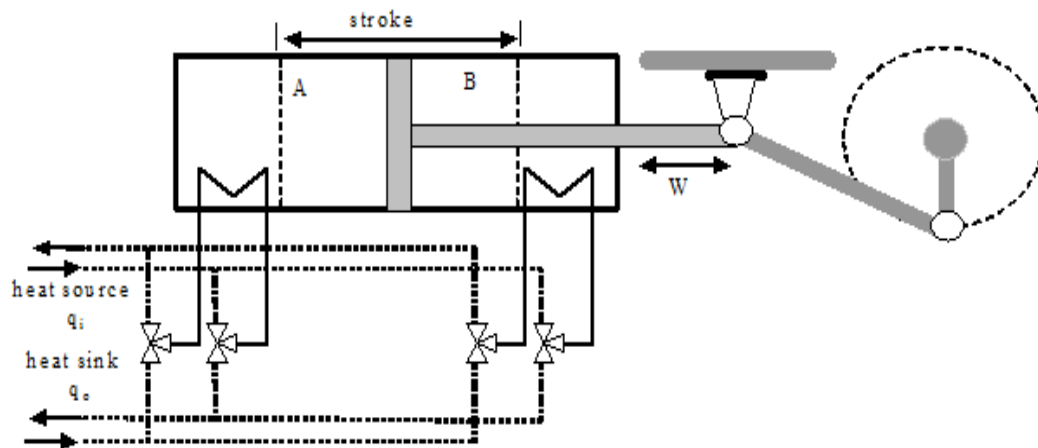


**Fig9.** Reciprocating double effect cylinder, heated and cooled by means of a heat source and heat sink deriving from a crankshaft.

### The Analysis of the Quadrilateral NCTC Undergoing Closed Polytropic Path Functions

Performing the analysis of the NCTC undergoing polytropic ideal processes along the cylinder stroke is a tedious task that could be approached only when subjected to serious constraints imposed by the inherent irreversibilities associated to any real thermal cycle. The cases that could yield acceptable ideal thermal efficiency are being considered, are those undergoing polytropic path functions. Fig. 9 depicts the schematic double effect cylinder with single heat exchangers used as heaters and coolers. The double effect cylinder is subjected to polytropic path functions under the corresponding mechanical load to satisfy the analysed path functions. The necessary condition to ensure a polytropic path function of  $PI = n$  along the cylinder stroke requires that the piston load reacting against the force exerted by the cylinder pressure at any point of the cylinder stroke follows the path defined by

$$p = \frac{p_1 \cdot V_1^n}{V^n} \quad (28)$$

Since, a polytropic path function obeys

$$p \cdot V^n = p_1 \cdot V_1^n = C \quad (29)$$

Where, the variable force exerted on the piston is a function of the piston position along the full piston stroke, given by  $F = p \cdot A = \frac{p_1 \cdot V_1^n}{V^n} \cdot A$ , with  $F$  being the force and  $A$  the cross-sectional area of the piston.

Table 1 shows the heat flow direction, the activity of the path function, the path function type, the polytropic index followed by the path function of both sides of the double effect cylinder. As shown in Table 1, the polytropic index is different depending on the direction of the heat flow. Thus, the value selected for the  $PI = n = -1.675$  at transition (2)-(3) corresponds to the expansion of the working fluid, while the  $PI = n = -1.761$  at transition (4)-(1) corresponds to the contraction of the working fluid. Both  $PI$  values have been chosen to optimise the thermal efficiency of the cycle. That is, the thermal efficiency is the maximum achievable with helium as the working fluid.

**Table1.** The heat flow direction for the NCTC composed of two isochoric and two polytropic transformations with  $n = -1.761$ , and  $n = -1,675$ .

Cylinder side A					Cylinder side B				
(i)-(i+1)	heat	work	process	PI	(i)-(i+1)	heat	work	process	PI
(1)-(2)	qi	no	Isochoric	$\infty$	(3)-(4)	qo	no	Isochoric	$\infty$
(2)-(3)	qi	yes	polytropic	-1.675	(4)-(1)	qo	yes	polytropic	-1.761
(3)-(4)	qo	no	Isochoric	$\infty$	(1)-(2)	qi	no	Isochoric	$\infty$
(4)-(1)	qo	yes	polytropic	-1.761	(2)-(3)	qi	yes	polytropic	-1.675

The data used in the cycle composed of two polytropic transformations and two isochoric transformations is shown in Table 2, for both

sides of the cylinder. The presented data has been used to calculate the thermal efficiency and the specific work. As can be observed that both

## Analysis and Comparison of Closed System Based Thermal Cycles Undergoing Different Polytropic Transformations

the top and bottom temperatures are abnormally low (330 K-290 K) in comparison with **Table 2**. The double effect cylinder performing mechanical work under two isochoric and two polytropic legs, showing for each state point (i) the corresponding temperature, pressure, specific volume, the entropy and the internal energy.

quadrilateral Carnot based thermal cycles.

Cylinder side A						Cylinder side B					
State i	T(K)	p (kPa)	v (m <sup>3</sup> /kg)	s (kJ/kg.K)	u (kJ/kg)	State i	T(i)(K)	p(i) (kPa)	v(i) (m <sup>3</sup> /kg)	s(i) (kJ/kg-K)	u(i) (kJ/kg)
1A	290	95	6.34	31.5	-644.7	1B	330	105	6.528	31.97	-520
2A	305.3	100	6.34	31.66	-597.1	2B	314.3	100	6.528	31.81	-569
3A	330	105	6.528	31.97	-520	3B	290	95	6.34	31.5	-644.7
4A	314.3	100	6.528	31.81	-569	4B	305.3	100	6.34	31.66	-597.1

The corresponding p-V diagram for helium is shown in Fig. 10.

Since both sides A and B of the cylinder operate under a symmetric profile with respect to the parameters shown in Tables 1 and 2, only the p-V diagram of side A is depicted.

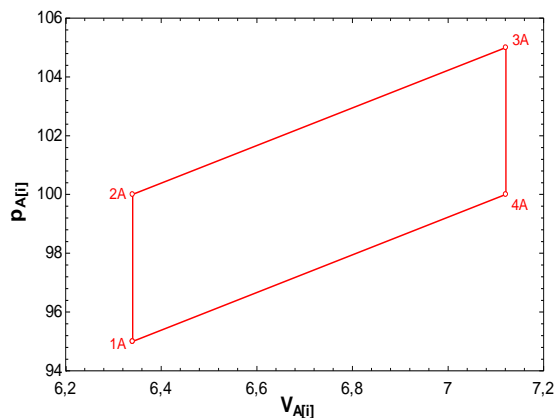


**Fig10.** The p-V diagram of the NCTC operating with the data of Tables 1 and 2, with helium as the working fluid.

### DISCUSSION OF RESULTS

The analysed cycle operating with Table 2 data yields the results shown in Fig. 11, where the ideal thermal efficiency and specific work for helium is shown. According to the obtained results, as consequence of the analysis carried out, the unusually high thermal efficiency achieved at low temperatures it is truly remarkable, from a theoretic perspective.

At such low top temperatures the Carnot factor is also low, so that the achieved thermal efficiency may be even higher than the Carnot factor at the same temperatures.

With regard to Fig. 11, it is noteworthy observing the thermal efficiency profile according to the above temperature range, it is highlighted that the slope tends to be canceled as a result of its low dependence on the temperature.

However, the specific work is linearly dependent on the top temperature.

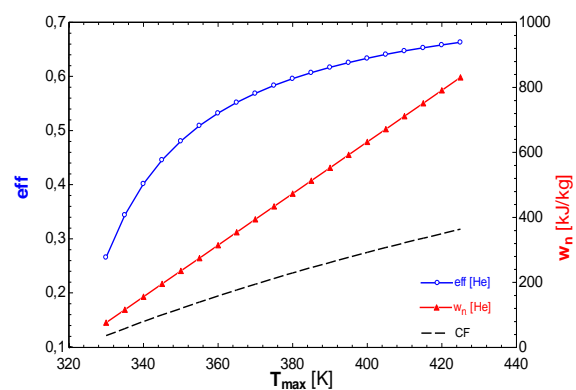


**Fig11.** The thermal efficiency and specific work of the NCTC, operating with helium as the working fluid together with Table 2 data, under polytropic path functions.

### CONCLUSIONS

The proposed NCTC has been studied for helium as the working fluid, although any other gas with acceptable characteristics would be useful since efficiency is a function which strongly depends on the polytropic indexes. According to the characteristics of the proposed NCTC, new expressions for the ideal thermal efficiency have been achieved and analysed.

The performance results of the NCTC have been compared with the results obtained for the Carnot cycle, operating between both the same range and ratio of temperatures.

The most relevant conclusion involves:

- The cycle processes of the NCTC, which is structured under closed system based transformations and,
- The thermal efficiency of the cycle which exceeds the Carnot efficiency under appropriate operating conditions.
- The maximum thermal efficiency is a function of the polytropic index, regardless

## Analysis and Comparison of Closed System Based Thermal Cycles Undergoing Different Polytropic Transformations

of the pressure ratios and operating temperatures.

- The cycle can operate at a very low temperature, even rendering high thermal efficiency in comparison with that of the Carnot factor.

The reason for this obeys the fact that in a cycle, polytropic heat absorption and simultaneous conversion into mechanical work and residual heat, take place simultaneously along a cycle transformation. Furthermore, thermal losses due to isentropic efficiency are avoided if reversible transformations can be approached. As revealed in the results, the ideal thermal efficiency is significantly increased in comparison with the conventional ORCs under feasible conditions. Finally, an overall conclusion concerns the fact that a new family of efficient thermal power plants at low temperatures, which are not restricted by the Carnot factor, is possible.

### REFERENCES

- [1] Johann Fischer, Comparison of trilateral cycles and organic Rankine cycles, *Energy*, 36 (2011) 6208-6219, <http://dx.doi.10.1016/j.energy.2011.07.041>;
- [2] S.C. Kaushik, V.SivaRedd, S.K.Tyagi, Energy and exergy analyses of thermal power plants: A review, *Renewable and Sustainable Energy Reviews*, 15 (2011)1857-1872.
- [3] Jing Li, Gang Pei, Yunzhu Li, Dongyue Wang, Jie Ji, Energetic and exergetic investigation of an organic Rankine cycle at different heat source temperatures, *Energy*, 38 (2012)85-95.
- [4] Yamamoto T, Furuhashi T, Arai N, Mori K, Design and testing of the Organic Rankine Cycle, *Energy*, 26 (2001)239-251.
- [5] Donghong Wei, Xuesheng Lu, Zhen Lu, Jianming Gu. Performance analysis and optimization of Organic Rankine Cycle (ORC) for waste heat recovery, *Energy Conversion and Management*, 48 (2007)1113-1119.
- [6] Wagar W.R., Zamfirescu C., Dincer I., Thermodynamic performance assessment of an ammonia–water Rankine cycle for power and heat production, *Energy Conversion and Management*, 51(2010) 2501-2509.
- [7] Saleh B, Koglbauer G, Wendland M, Fischer J, Working fluids for low temperature Organic Rankine Cycles, *Energy*, 32(7) (2006)1210-1221.
- [8] Hung T, Waste heat recovery of Organic Rankine Cycle using dry fluids, *Energy Conversion and Management*, 42 (2001)539-553.
- [9] Xiaohui She, Yonggao Yin , Xiaosong Zhang, Thermodynamic analysis of a novel energy-efficient refrigeration system subcooled by liquid desiccant dehumidification and evaporation, *Energy Conversion and Management* 78 (2014)286–296
- [10] E. W. Lemmon, M. L. Huber and M. O. Mc Linden. NIST Reference Fluid Thermodynamic and Transport Properties - REFPROP Version 8.0, User's Guide, NIST 2007, Boulder, Colorado.

**Citation:** Ramon Ferreiro. Garcia, Jose Carbia Carril, “Analysis and Comparison of Closed System Based Thermal Cycles Undergoing Different Polytropic Transformations”, *International Journal of Emerging Engineering Research and Technology*, 7(1), pp.26-37

**Copyright:** © 2019 Ramon Ferreiro. Garcia. This is an open-access article distributed under the terms of the Creative Commons Attribution License, which permits unrestricted use, distribution, and reproduction in any medium, provided the original author and source are credited.